(LNS Experiment : #2534, #2576)

# Performance of the Tagging System for GeV-$\gamma$ Beamline STB-Tagger II

T. Ishikawa[1], T. Fujibayashi[2], H. Fujimura[1], H. Fukasawa[1], R. Hashimoto[1], T. Iwata[3], H. Kanda[2], J. Kasagi[1], H. Kato[3], T. Kinoshita[1], M. Itoh[4], K. Maeda[2], M. Matsuzawa[2], T. Michigami[3], F. Miyahara[1], K. Mochizuki[1], K. Murakami[3], T. Nakabayashi[1], K. Nawa[1], T. Nomura[3], K. Okamura[1], H. Okamura[5], H. Okuyama[3], Y. Onodera[1], Y. Saitoh[1], T. Sasaki[3], M. Sato[1], H. Shimizu[1], T. Shishido[3], S. Suzuki[1], K. Suzuki[1], Y. Tajima[3], T. Takahashi[6], S. Takita[3], H. Ueno[3], H.Y. Yoshida[3], S. Yamaguchi[3], and H. Yamazaki[1]

[1]*Laboratory of Nuclear Science, Tohoku University, Sendai 982-0826*
[2]*Department of Physics, Tohoku University, Sendai 980-8578*
[3]*Department of Physics, Yamagata University, Yamagata 990-8560*
[4]*Cyclotron and Radioisotope Center, Tohoku University, Sendai 980-8578*
[5]*Research Center for Nuclear Physics, Osaka University, Ibaraki 567-0047*
[6]*High Energy Accelerator Research Organization (KEK), Tsukuba 305-0801*

High energy photons shed light on nucleon resonances by measuring produced mesons on the nucleon. In the GeV-$\gamma$ beamline [1], bremsstrahlung photons are used as a beam, which are generated by inserting a carbon fiber (radiator) into circulating electrons on the STretcher Booster (STB) ring. A tagging system has been constructed to determine the energy of the photon associating with the meson produced event measured by a detector system on the beamline.

The STB-Tagger II consists of 116 telescopes of two scintillating fibers, and each telescope (tagger) determines the trajectories of momentum-analyzed electrons which lose energy due to bremsstrahlung at the radiator. The photon energy is determined from the difference of energies of the circulating and recoil electrons. Details of the STB-Tagger II are described elsewhere [2]. The tagging energy of each tagger is reported in the internal notes [3]. A part of the tagging energy calibration is also presented in a research report of LNS [4]. In this report, the transmission rate of the photon, a low energy component of the tagged photon, and a fraction of tagged photons to all the incident ones will be described.

## §1. Transmission Rate

Some electrons which do not generate a photon caused by

1. Møller scattering,
2. Coulomb multiple scattering on the radiator or the gas particle in the vacuum chamber, and
3. unstability of the circulating beam in the STB ring

come into the STB-Tagger II. Even if photons are generated, they may not come to the target position due to

1. large difference in direction between the generated photons and the beamline, and
2. conversion to positron and electron pairs with materials on the beamline.

The transmission rate is defined as a ratio of the number of associating photons coming to the target position to the number of electrons that each tagger responds to. It is experimentally measured since it is difficult to incorporate all the status of circulating electrons in the calculation.

The energy of incident photons is measured with an SF-5 lead glass Čerenkov counter with a size of 150 mm (W) $\times$ 150 mm (H) $\times$ 300 mm [5]. Undesirable charged particles in the beam are swept out with a dipole magnet $\mathcal{R}$TAGX [6]. The trigger for the data taking system is an OR signal of the STB-Tagger II. The transmission rate for the $i$-th tagger $T_i$ is obtained as

$$T_i = \frac{N_i^{\gamma}}{N_i}, \tag{1}$$

where $N_i$ is the number of signals from the $i$-th tagger and $N_i^{\gamma}$ is the number of coincidences between the $i$-th tagger and the SF-5 counter with the corresponding photon energy. Figure 1 shows a sample of the measured transmission rate. The details of determining the transmission rate are described elsewhere [7].

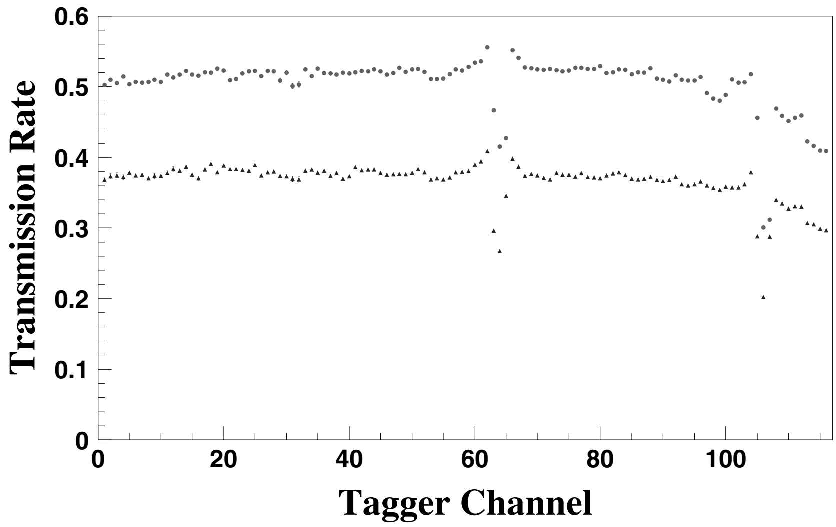


Fig.1. Measured transmission rate. The circles show the transmission rate for 1200 MeV circulating electron beam, and the triangles shows that for 920 MeV one.

The transmission rate as a function of the tagger channel shows two dips. These dips correspond to the taggers to which supporting rods lie on the central orbit of ongoing electrons. The vacuum chamber of the STB ring in the BM5 has a Ti window with a thickness of 50 $\mu$m to introduce post bremsstrahlung electrons into taggers. Two rods made of SUS support the window frame. The post bremsstrahlung electrons impacting against these rods are not detected with the STB-Tagger II.

The circulating electrons have various momentum vectors at the radiator point. Some electrons generating bremsstrahlung photons take different courses and are detected with the STB-Tagger II. The corresponding photons are blocked with a lead aperture. These events deteriorate the transmission rate, and make two dips in that as a function of the tagger channel. Figure 2 shows how the transmission rate is deteriorated for the taggers which are shaded with the supporting rods.

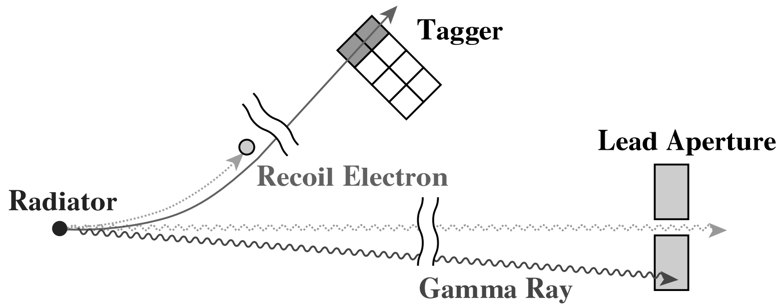


Fig.2. How the transmission rate is deteriorated for the taggers which are shaded with the supporting rods. The photons generated by inclined electrons do not come to the target point, while the post bremsstrahlung electrons do not hit the rods and are detected with the STB-Tagger II.

The transmission rate is estimated with a Monte Carlo calculation, and the measured one is qualitatively reproduced. Figure 3 shows the transmission rate estimated with the calculation. Its shape in the lower channel region is determined by an effect of Møller scattering electrons. Most of the Møller scattered electrons are blocked with an iron fence (field cramp) [8] for the reducing leakage magnetic flux in the region where photo-multiplier tubes of the STB-Tagger II are placed.

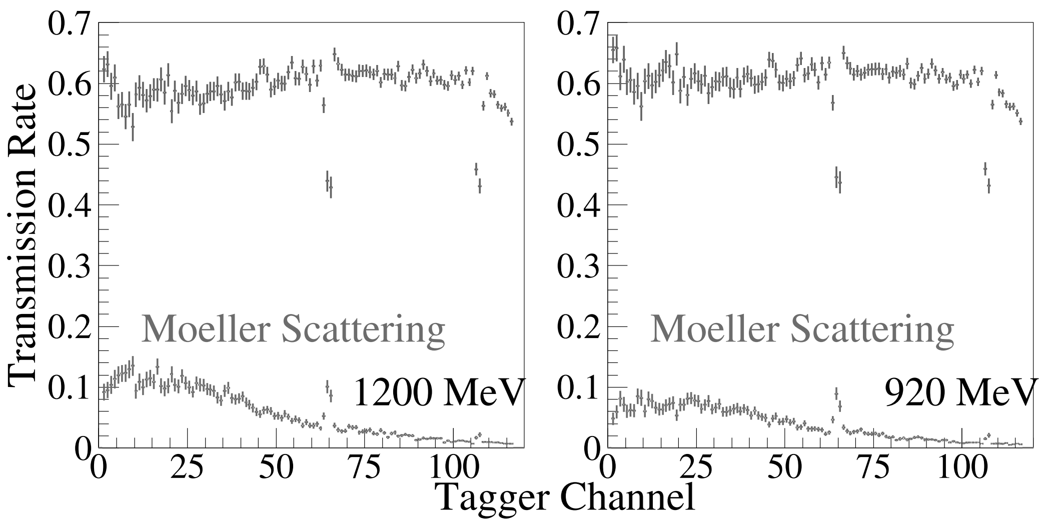


Fig.3. Transmission rate estimated with a Monte Carlo calculation. The left and right panels show the transmission rates for 1200 and 920 MeV circulating electron beams, respectively. The upper points show the transmission rate and the lower show the Møller scattering effects. The transmission rate obtained by the calculation qualitatively reproduces the measured one.

## §2. Low Energy Component of Tagged Photons

The measured energy of incident photons shows a low energy component for the tagging channels larger than 102 [9]. This low energy component has been a long standing problem on the STB-Tagger II,

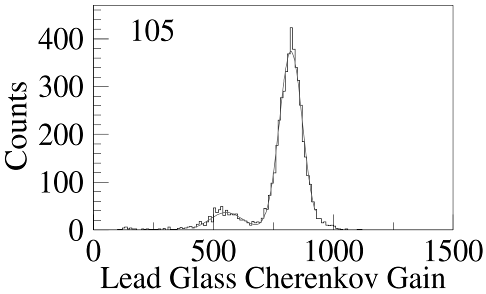


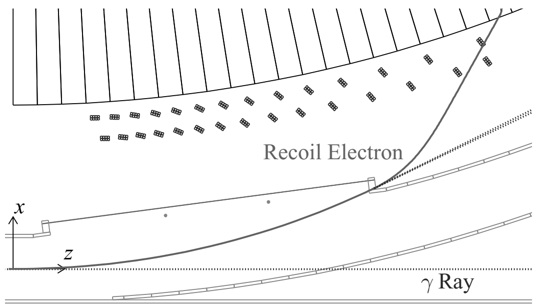


Fig.4. Events with post bremsstrahlung electrons impacting against the frame of the Ti window. The energy of the generating photons is lower than that of the nominal tagged photons. The left panel shows the ADC distribution for the 105-th tagging channel, and the right one shows the trajectories of generated particles in such a event.

and a Monte-Carlo simulation has revealed its source. Some post bremsstrahlung electrons impacting against the frame of the Ti window are detected with the STB-Tagger II. These electrons are mainly detected with the tagging channel larger than 102, and the energy of the corresponding photons is lower than that of the nominal tagged photons. Figure 4 shows the events with post bremsstrahlung electrons impacting against the frame of the Ti window.

## §3. Fraction of Tagged Photons

A fraction of tagged photons to all the incident ones was measured with the SF-5 counter located on the GeV-$\gamma$ beamline. In the first step, the energy of the counter was measured where the trigger for the data taking system was the OR signal of the STB-Tagger II. Energy calibration was made by using these data so that the measured energy should be the incident photon one corresponding to the tagging channel. Only the tagged photons without the low energy component were used in the calibration. Figure 5 shows the mean of the ADC distribution as a function of the tagging energy. The photon energy was obtained from the ADC value $A$ as

$$E_\gamma = \frac{A - 78.87 \pm 0.01}{1.3202 \pm 0.0001}. \qquad (2)$$

In the next step, the energy was measured with the SF-5 counter where the trigger was the signal of the counter itself. Figure 6a) shows the energy distribution measured with the SF-5 counter together with that in coincidence with STB-Tagger II, and Figure 6b) shows a fraction of tagged photons as a function of the energy measured with the SF-5 counter. Fractions of tagged photons in the photon energy raging from 800 to 1100 MeV are about 65%. A fraction of all the tagged photons to all the photons detected with the SF-5 counter were 7.22%.

Number of incident photons measured with the SF-5 counter depends on the threshold value of its discriminator. The energy distribution was fitted from 0 to 1000 MeV with a function as

$$f(E_\gamma) = (5.91 \pm 0.02)\,\mathrm{freq}\left(\frac{x - 33.12 \pm 0.04}{9.23 \pm 0.03}\right) E_\gamma^{-1.149} \qquad (3)$$

where freq stands for the Gaussian convoluted step function [11]. The threshold values were found to be corresponding to $33.12 \pm 0.04$ MeV. Number of incident photons with the energy less than discriminator

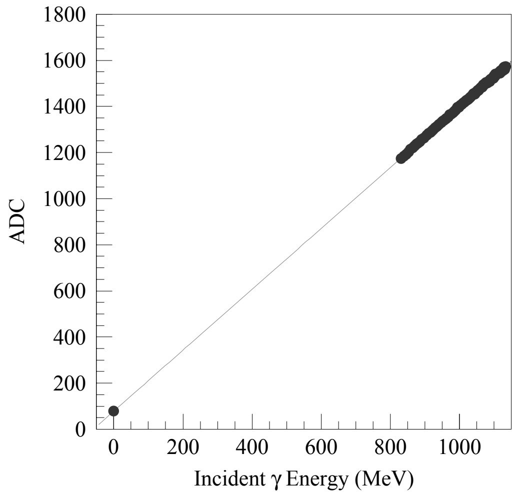


Fig.5. Mean of the SF-5 ADC distribution as a function of the tagging energy. The solid curve shows the function (2).

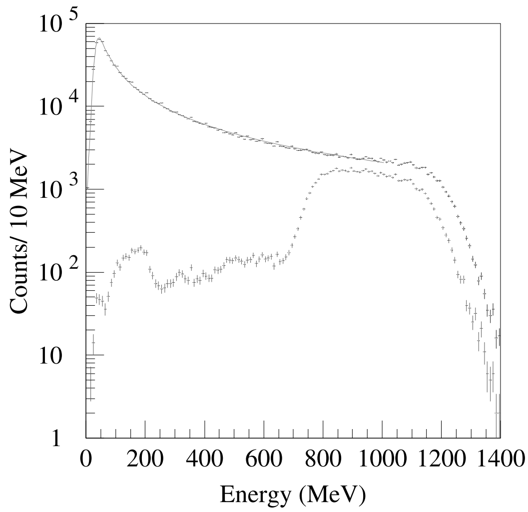


Fig.6. a) Energy distribution of the SF-5 counter. The upper histogram shows the energy distribution and the lower shows that coincidence with STB-Tagger II. The solid curve shows the fitted function (3). b) Fraction of tagged photons as a function of the energy measured with the SF-5 counter.

threshold were deduced as an integration of a function

$$f(E_\gamma) = (5.91 \pm 0.02)\, E_\gamma^{-1.149}, \tag{4}$$

from $2m_e$ to the threshold value where $m_e$ denotes the mass of the electron. The number of all the incident photons were given by summing the numbers of photons detected with the SF-5 counter and photons with the energy less than the threshold. A fraction of all the tagged photons to all the incident photons was obtained to be 2.78%. The details of the analysis are described elsewhere [12].

## References


[1] H. Shimizu *et al.*: Research Report of LNS, Tohoku University **37** (2004) 13.

[2] T. Nakabayashi *et al.*: Research Report of LNS, Tohoku University **37** (2004) 17.

[3] T. Ishikawa: Internal GeV-$\gamma$ Analysis Note No. **15** (2006);
T. Ishikawa: Internal GeV-$\gamma$ Analysis Note No. **23** (2006);
T. Ishikawa: Internal GeV-$\gamma$ Analysis Note No. **24** (2006);
T. Ishikawa: Internal GeV-$\gamma$ Analysis Note No. **25** (2006);
K. Suzuki: Internal GeV-$\gamma$ Analysis Note No. **35** (2006–2007);
T. Ishikawa: Internal GeV-$\gamma$ Analysis Note No. **55** (2007);
T. Ishikawa: Internal GeV-$\gamma$ Analysis Note No. **57** (2007);
K. Suzuki: Internal GeV-$\gamma$ Analysis Note No. **59** (2007);
T. Ishikawa: Internal GeV-$\gamma$ Analysis Note No. **60** (2007).

[4] K. Suzuki *et al.*: Research Report of LNS, Tohoku University **40** (2007) 10.

[5] M. Sato and T. Ishikawa *et al.*: in this Research Report of LNS, **41** (2008) 22;
M. Sato: Internal GeV-$\gamma$ Analysis Note No. **86** (2008).

[6] T. Ishikawa *et al.*: Research Report of LNS, Tohoku University **39** (2006) 39.

[7] T. Nakabayashi: Internal GeV-$\gamma$ Analysis Note No. **29** (2006);
T. Ishikawa: Internal GeV-$\gamma$ Analysis Note No. **31** (2006);
F. Miyahara: Internal GeV-$\gamma$ Analysis Note No. **88** (2008).

[8] T. Nakabayashi *et al.*: Research Report of LNS, Tohoku University **37** (2004) 17;
T. Ishikawa: Internal GeV-$\gamma$ Analysis Note No. **24** (2006);
T. Ishikawa: Internal GeV-$\gamma$ Analysis Note No. **25** (2006).

[9] T. Nakabayashi: Internal GeV-$\gamma$ Analysis Note No. **14** (2006);
T. Ishikawa: Internal GeV-$\gamma$ Analysis Note No. **15** (2006).

[10] T. Ishikawa: Internal GeV-$\gamma$ Analysis Note No. **61** (2007).

[11] Computing and Networks Division, CERN Program Library Office: CERNLIB — CERN Program Library Short Writeups (1996).

[12] T. Ishikawa: Internal GeV-$\gamma$ Analysis Note HD No. **125**$\mathcal{T}$ (2009).